

# Indirect exchange in GaMnAs bilayers via spin-polarized inhomogeneous hole gas: Monte Carlo simulation

M. A. Boselli, I. C. da Cunha Lima

*Instituto de Física, Universidade do Estado do Rio de Janeiro*

*Rua São Francisco Xavier 524, 20.500-013 Rio de Janeiro, R.J., Brazil*

A. Ghazali

*Groupe de Physique des Solides, Universités Paris 6 et Paris 7*

*Tour 23, 2 Place Jussieu, F-75 251 Paris Cedex 05, France*

(Dated: October 29, 2018)

## Abstract

The magnetic order resulting from an indirect exchange between magnetic moments provided by spin-polarized hole gas in the metallic phase of a  $\text{Ga}_{1-x}\text{Mn}_x\text{As}$  double layer structure is studied *via* Monte Carlo simulation. The coupling mechanism involves a perturbative calculation in second order of the interaction between the magnetic moments and carriers (holes). We take into account a possible polarization of the hole gas due to the existence of an average magnetization in the magnetic layers, establishing, in this way, a self-consistency between the magnetic order and the electronic structure. That interaction leads to an internal ferromagnetic order inside each layer, and a parallel arrangement between their magnetizations, even in the case of thin layers. This fact is analyzed in terms of the inter- and intra-layer interactions.

## I. INTRODUCTION

During the last decade a new interest arose in the study of the magnetic order in layered materials. This area includes the study of magnetic semiconductor pseudo-binary alloys like  $A_{1-x}M_xB$ , where M stands for a magnetic ion. These alloys are called Diluted Magnetic Semiconductors (DMS).<sup>1,2</sup> A few years ago some groups<sup>3,4,5,6,7,8,9</sup> succeeded in producing homogeneous samples of  $Ga_{1-x}Mn_xAs$  alloys with  $x$  up to 7% using low temperature (200 – 300° C) Molecular Beam Epitaxy (MBE) techniques. Mn is a transition metal having its  $3d$  level half filled with five electrons, in such a way that it carries a spin of  $5\hbar/2$ , according to the Hund's rule. In  $Ga_{1-x}Mn_xAs$  alloys a substitutional Mn acts as an acceptor (it binds one hole), and at the same time it carries a localized magnetic moment, due to its  $3d$  shell. For  $x = 0.053$ , the alloy is a metallic ferromagnet,<sup>7</sup> the Curie-Weiss temperature is 110K, and the free hole concentration is near  $1 - 2 \times 10^{20} \text{ cm}^{-3}$ . The ferromagnetic order in the metallic phase is understood as resulting from the indirect exchange between the Mn ions due to the local spin polarization in the hole gas.<sup>10</sup> At present a vast literature exists about different possible mechanisms for that indirect exchange.<sup>10,11,12,13</sup> The free hole concentration in the metallic phase is a fraction (10-20%) of the total concentration of Mn. This is understood as due to the presence of As anti-sites and interstitial Mn. The magnetic ordering resulting from indirect exchange *via* spin-polarized free carriers implies in a spin coherence length larger than the average distance between localized magnetic moments. The possibility of having a DMS based on GaAs opens a wide range of potential applications as, for instance, in integrated magneto-optoelectronic devices.<sup>14</sup>

In this work we extended a confinement-adapted Ruderman-Kittel-Kasuya-Yosida (RKKY)<sup>10</sup> mechanism to study the magnetic order resulting from the indirect exchange between magnetic moments in a GaAs/ $Ga_{1-x}Mn_xAs$  nanostructure with two DMS layers. A temperature dependent Monte Carlo (MC) simulation is performed to determine the resulting magnetic phases. This article is organized as follows. In Sec. II we present the calculation of the indirect exchange for a confined spin-polarized Fermi gas in a semiconductor heterostructure. In Sec. III the self-consistent calculation of the heavy-hole single band electronic structure is presented in some detail. In Sec. IV the Monte Carlo simulation is performed to determine the resulting magnetic phases and the relevant properties. In Sec. V we present our conclusions. Our calculations reveal that a ferromagnetic phase exists even

in thin layers in the structure containing two DMS layers. Considering the intra-layer and the inter-layer interactions as two independent mechanisms, we conclude that the intra-layer interaction is dominant in what concerns the internal magnetic order of each layer, while the inter-layer interaction alone, which determines the relative orientation of the two average magnetizations, is responsible for a transition temperature four times lower than that resulting from the two mechanism acting together. The roles of the carrier concentration and of the cutoff parameter are also analyzed.

## II. INDIRECT EXCHANGE VIA SPIN-POLARIZED FERMI GAS

The indirect exchange between localized magnetic moments in quasi-two-dimensional structures mediated by a Fermi gas has been addressed several times.<sup>15,16,17,18,19,20,21,22</sup> Basically, it deals with a confined electron (or hole) gas being locally spin-polarized by magnetic moments distributed in a layer.

The interaction potential between the Fermi gas and the set of localized magnetic moments is well described by the Kondo-like exchange term:

$$H_{\text{ex}} = -I \sum_i \vec{S}_i \cdot \vec{s}(\vec{r}) \delta(\vec{r} - \vec{R}_i), \quad (1)$$

where the localized spin of the Mn ion  $\vec{S}_i$  at position  $\vec{R}_i$  will be treated as a classical variable, and  $\vec{s}(\vec{r})$  is the spin operator of the carrier at position  $\vec{r}$ ;  $I$  is the  $sp - d$  interaction.

If  $\hat{\psi}_\sigma(\vec{r})$  and  $\hat{\psi}_\sigma^\dagger(\vec{r})$  describe the fermion field operator for spin  $\sigma$ , then

$$s^z(\vec{r}) = \frac{1}{2} (\hat{\psi}_\uparrow^\dagger(\vec{r}) \hat{\psi}_\uparrow(\vec{r}) - \hat{\psi}_\downarrow^\dagger(\vec{r}) \hat{\psi}_\downarrow(\vec{r})), \quad (2)$$

$$s^+(\vec{r}) = \hat{\psi}_\uparrow^\dagger(\vec{r}) \hat{\psi}_\downarrow(\vec{r}), \quad (3)$$

$$s^-(\vec{r}) = \hat{\psi}_\downarrow^\dagger(\vec{r}) \hat{\psi}_\uparrow(\vec{r}), \quad (4)$$

with the usual definitions of  $s^+ = s_x + is_y$ , and  $s^- = s_x - is_y$ . In terms of field operators, the (Kondo) exchange term in the Hamiltonian is

$$H_{\text{ex}} = -\frac{I}{2} \sum_i \{ S_i^z [\psi_\uparrow^\dagger(\vec{r}_i) \psi_\uparrow(\vec{r}_i) - \psi_\downarrow^\dagger(\vec{r}_i) \psi_\downarrow(\vec{r}_i)] + S_i^+ \psi_\downarrow^\dagger(\vec{r}_i) \psi_\uparrow(\vec{r}_i) + S_i^- \psi_\uparrow^\dagger(\vec{r}_i) \psi_\downarrow(\vec{r}_i) \}. \quad (5)$$

We consider holes in a semiconductor heterostructure that are confined in the growth direction, assumed to be the  $z$ -axis. The total Hamiltonian,  $H = H_0 + H_{\text{ex}}$  includes in  $H_0$  the kinetic part, the confinement potential and the Hartree as well as exchange and correlation terms.<sup>23</sup> Neglecting scattering from impurities, holes in the effective mass approximation are free particles in the  $(x, y)$  plane, i.e., in the plane parallel to the layer interfaces. Their field operator can be written as

$$\hat{\psi}_\sigma(\vec{r}) = \frac{1}{\sqrt{A}} \sum_{n, \vec{k}} e^{i\vec{k} \cdot \vec{r}} \phi_{n, \sigma}(z) \eta_\sigma c_{n, \vec{k}, \sigma}, \quad (6)$$

where  $A$  is the normalization area,  $\vec{k}$  is a wave vector in the  $(x, y)$  plane,  $\eta_\sigma$  is the spin tensor for the polarization  $\sigma$ ,  $\phi_{n, \sigma}(z)$  is the envelope function which describes the motion of the fermion in the  $z$ -direction, and  $c_{n, \vec{k}, \sigma}$  is the fermion annihilation operator for the state  $(n, \vec{k}, \sigma)$ .  $\vec{r}$  represents a vector in the  $(x, y)$  plane.

The confined RKKY indirect exchange is a second-order perturbative treatment. It gives two terms for the correction to the ground state energy of the system formed by the set of (classical) localized moments and the Fermi gas.<sup>10</sup> The first one is the self-energy term, which corrects the site energy. The second is the interaction between the localized magnetic moments, the RKKY exchange, allowing the interaction to be written as a Heisenberg Hamiltonian:

$$\delta E^{(2)} = - \sum_{i, j} J_{ij} \mathbf{S}_i \cdot \mathbf{S}_j. \quad (7)$$

The RKKY approach can be extended to spin-polarized states. This is, in one sense, going beyond the second-order perturbation. In that case no simple spin-spin scalar product is obtained, as in Eq. (7), since the spin polarization breaks the rotational symmetry establishing a preferential direction, namely that of the average magnetization.

In the second-order perturbation, the correction to the energy which is bilinear in the magnetic ion dipole moment is obtained from

$$\delta E^{(2)} = - \sum_{t', F'} \frac{\langle F, t | H_{\text{ex}} | F', t' \rangle \langle F', t', | H_{\text{ex}} | F, t \rangle}{E_{F', t'}^0 - E_{F, t}^0}. \quad (8)$$

Here, the state  $|F, t\rangle$  is understood as the direct product of the state of the system of classical localized moments and that of the quantum spin-polarized gas. Substituting Eq. (5) into Eq. (8) we obtain, after a lengthy calculation, the effective Hamiltonian which includes

explicitly the spin-flip terms:

$$H_{eff} = - \sum_{i,j} (C_{ij}^{\uparrow\uparrow} + C_{ij}^{\downarrow\downarrow}) S_i^z S_j^z + (C_{ij}^{\uparrow\downarrow} + C_{ij}^{\downarrow\uparrow}) (S_i^x S_j^x + S_i^y S_j^y), \quad (9)$$

where the spin-flip term is given by:

$$C_{ij}^{\uparrow\downarrow} = - \sum_{n \in \uparrow} \sum_{n' \in \downarrow} \sum_{\mathbf{k}, \mathbf{q}} \left( \frac{I}{2A} \right)^2 \frac{1}{\epsilon_{n', \mathbf{k} + \mathbf{q}} - \epsilon_{n, \mathbf{k}}} \exp[i\mathbf{q}(\mathbf{R}_j - \mathbf{R}_i)] \times \phi_{n'}^*(z_i) \phi_n(z_i) \phi_{n'}^*(z_j) \phi_{n'}(z_j) \theta(E_F - \epsilon_{n, \mathbf{k}}) \theta(\epsilon_{n', \mathbf{k} + \mathbf{q}} - E_F). \quad (10)$$

Notice that the arrows refer to spins up or down for holes, not the orientation of the localized magnetic moments at the Mn sites. Similar definitions hold for the other  $C_{ij}^{\sigma\sigma'}$ . Eq. (10) can be expressed in terms of the Lindhard function:<sup>24,25</sup>

$$\chi^{n, n'}(\vec{q}) = \sum_{\vec{k}} \frac{\theta(E_F - \epsilon_{n, \vec{k}}) - \theta(E_F - \epsilon_{n', \vec{k} + \vec{q}})}{\epsilon_{n', \vec{k} + \vec{q}} - \epsilon_{n, \vec{k}}}, \quad (11)$$

and its real-space Fourier transform:

$$\chi^{n, n'}(\mathbf{R}_{ij}) = \sum_{\vec{q}} \exp[-i\vec{q} \cdot \mathbf{R}_{ij}] \chi^{n, n'}(\vec{q}). \quad (12)$$

Substituting Eq. (11) in Eq. (10) we obtain

$$C_{ij}^{\mu\nu} = - \sum_{n \in \mu} \sum_{n' \in \nu} \left( \frac{I}{2A} \right)^2 \phi_{n'}^*(z_i) \phi_n(z_i) \phi_{n'}^*(z_j) \phi_{n'}(z_j) \chi^{n, n'}(\mathbf{R}_{ij}), \quad (13)$$

where the summations on  $n$  and  $n'$  are restricted to those sub-bands with the proper spin polarization.

The intra-subband real space Lindhard function  $\chi^{n, n}(\mathbf{R}_{ij})$  has been derived by several authors.<sup>10,15,18,19,20</sup>

$$\chi^{n, n}(R_{ij}) = - \frac{m_t^* A^2}{4\pi\hbar^2} k_F^{(n)2} [J_0(k_F^{(n)} R_{ij}) N_0(k_F^{(n)} R_{ij}) + J_1(k_F^{(n)} R_{ij}) N_1(k_F^{(n)} R_{ij})], \quad (14)$$

where  $m_t^*$  is the transversal (parallel to the interfaces) effective mass, and  $k_F^{(n)}$  refers to the Fermi wavevector of subband  $n$ .

The inter-subband terms cannot be expressed in a closed form.<sup>10</sup> They must be obtained numerically from the integral

$$\chi^{n, n'}(\mathbf{R}_{ij}) = - \int_0^\infty dq q F_{n, n'}(q) J_0(q R_{ij}), \quad (15)$$

where

$$F_{n, n'}(q) = \frac{A^2 m_t^*}{8\pi^2 \hbar^2} \left( 1 - \frac{\Delta_{n', n}}{q^2} \right) \left[ 1 - \sqrt{1 - \left( \frac{2k_F^{(n)} q}{q^2 + \Delta_{n', n}} \right)^2} \right] \theta(q^2 + \Delta_{n', n} - 2qk_F^{(n)}) \theta(\epsilon_{n'} - E_F), \quad (16)$$

with  $\Delta_{n', n} = 2m_t^* \cdot (E_{n'} - E_n)/\hbar^2$ .

### III. SPIN-POLARIZED ELECTRONIC STRUCTURE FOR MAGNETIC MULTILAYERS

In order to obtain the spin-polarized electronic structure for holes given an average magnetization of the Mn ions, we solve self-consistently the heavy hole single band Schrödinger equation in the reciprocal space. The hole system is supposed to be homogeneous in the  $xy$  plane, so the Hartree term depends only on the coordinate  $z$ ,  $U_H(\vec{r}) = U_H(z)$ . For the purpose of obtaining the electronic structure we treat the magnetic interaction as being due to an uniform magnetization in the DMS layers. If a net magnetization exists, it will polarize the hole gas. This problem is solved self-consistently by a secular matrix equation in the reciprocal space. The method would be exact were not for cutting the matrix size. The advantage is that it provides spin-polarized eigenvalues and eigenfunctions with high accuracy, not only for bound states, but also for a high number of scattering states. For each spin, we define the wavefunction Fourier Transform (FT):

$$\psi_\sigma(\vec{r}) = \int d^3q \exp(i\vec{q} \cdot \vec{r}) \psi_\sigma(\vec{q}). \quad (17)$$

The hole eigenstates will be obtained by discretizing the integrals on  $\vec{q}$  appearing in

$$\int d^3r \psi_\sigma^*(\vec{r})(H - E)\psi_\sigma(\vec{r}) = 0. \quad (18)$$

When integrating the magnetic term in the Hamiltonian over  $\vec{r}$ , we assumed the magnetic impurities to be uniformly distributed in each one of the  $\text{Ga}_{1-x}\text{Mn}_x\text{As}$  DMS layers, all of them having the same thermal average magnetization. This treatment includes not only the ferromagnetic phase but also phases where a partial magnetization is observed, as the “canted-spin” phases.<sup>10,26</sup> Therefore, taking an homogenous concentration of  $N_i$  magnetic impurities in the  $j$ -th layer, we have:

$$\begin{aligned} & -I \int d^3r \exp[i(\vec{q} - \vec{q}') \cdot \vec{r}] \sum_j \sum_{i \in j}^{N_i} \vec{s}(\vec{r}) \cdot \vec{S}(\vec{R}_i) \delta(\vec{r} - \vec{R}_i) \simeq \\ & -I \frac{\sigma}{2} \sum_j \langle M \rangle_j \sum_{i \in j}^{N_i} \exp[i(\vec{q} - \vec{q}') \cdot \vec{R}_i] = \\ & -I \frac{\sigma}{2} \sum_j \langle M \rangle_j \frac{N_i}{V} \int d^3R_i \exp[i(\vec{q} - \vec{q}') \cdot \vec{R}_i] = \\ & -N_0 \beta \frac{\sigma}{2} x \sum_j \langle M \rangle_j F_{DMS}^j(q_z - q'_z) (2\pi)^3 \delta^2(\vec{q}_\parallel - \vec{q}'_\parallel), \end{aligned} \quad (19)$$

where  $\sigma = \pm 1$  for spin parallel (upper sign) or anti-parallel (lower sign) to the magnetization, and  $\frac{N_i}{V} = xN_0$  is the impurity density, in terms of  $N_0$ , the density of the cation ions. The  $sp$ - $d$  exchange constant for holes is usually written as  $\beta$ . Here we used  $N_0\beta = -1.2\text{eV}$ .<sup>27</sup>  $F_{DMS}^j$  is the integral performed on the  $z$ -coordinate inside the  $j$ -th DMS layer:

$$F_{DMS}^j(q) \equiv \frac{1}{2\pi} \int dz \exp[iq.z]. \quad (20)$$

Comparing Eqs. (19) and (20), the latter being just the Fourier transform of an unit barrier function within the range of the  $j$ -th DMS layer, we see that the thermal average magnetization  $\langle M \rangle_j$  polarizes the hole gas by introducing additional effective confining potentials given by

$$V_{mag}^{eff}(z) = -N_0\beta x \frac{\sigma}{2} \sum_j \langle M \rangle_j g_j(z), \quad (21)$$

where  $g_j(z) = 1$  if  $z$  lies inside the  $j$ -th layer, and  $g_j(z) = 0$  otherwise. Next, we define

$$U_{eff}(q) = \frac{1}{2\pi} \int dz \exp[iq.z] [U_c(z) + V_{mag}^{eff}(z) + U_H(z)], \quad (22)$$

where  $U_c(z)$  and  $U_H(z)$  are the confining and the Hartree potentials, respectively. The eigenvalues and eigenfunctions at the bottom of the 2-D subbands may be obtained by solving the secular equation for each spin polarization:

$$\det \left\{ \left[ \frac{\hbar^2 q_z^2}{2m^*} - E \right] \delta(q_z - q'_z) + U_{eff}(q_z - q'_z) \right\} = 0. \quad (23)$$

#### IV. MONTE CARLO SIMULATION: INTERLAYER INTERACTION AND MAGNETIC ORDERING

In the present work we have focused our attention on metallic systems with the Mn concentration  $x = 5\%$ , and we have neglected possible superexchange (anti-)ferromagnetic interaction between the nearest neighbors and the next-nearest neighbors pairs. We have performed extensive Monte Carlo (MC) simulations in order to determine the possible magnetic order occurring in a system containing a double layer of  $\text{Ga}_{1-x}\text{Mn}_x\text{As}$ . Classical spins  $\mathbf{S}_i$ , representing the localized magnetic moments of the Mn ions, are randomly distributed on the cation sites with concentration  $x$ . They are assumed to interact through the exchange Hamiltonian defined by Eq. (9).

The interaction derived in Sec. II is assumed to be effective within a cutoff radius which corresponds to the carrier spin coherence length. This cutoff is taken tentatively as  $R_c =$

$2.5a$ , and  $R_c = 2a$ , where  $a$  is the fcc lattice parameter of GaAs. These values correspond to five and four monolayers (ML), respectively. This choice makes the smallest value assumed for  $R_c$  nearly equal to the hole mean free path estimated from bulk transport measurements.<sup>7</sup>

The electronic structure was calculated for a system of two DMS layers grown inside a GaAs quantum well. We have studied two different DMS layer widths, 10 and 20 Å. The GaAs spacer separating the DMS layers has been considered as having widths varying from 5 Å to 60 Å. The whole system consists of a 200 Å quantum well with infinite barriers in the  $z$ -direction, in the center of which the two GaMnAs layers and a GaAs spacer are disposed, as shown in Fig. 1. The eigenstates, obtained according to Sec. III, were calculated for net magnetizations  $\frac{\langle M \rangle}{5\hbar/2} = 0.0, 0.1, 0.2, \dots, 1.0$ , for each one of the geometries used. Notice that  $\langle M \rangle$  determines the effective magnetic potential in Eq. (21) and, in consequence, the whole electronic structure. A typical result for the electric charge density, and the spin polarization densities is shown in Fig. 1c. We see that holes are attracted to the region of the DMS layers by the negatively charged Mn ions. Because  $N_0\beta$  is negative, however, the  $sp-d$  interaction (taken into account as the effective magnetic potential) favors the occurrence of anti-parallel spin subbands at lower energies. Several subbands are occupied, due to the high concentration of free carriers, most of them corresponding to the anti-parallel spin polarization. Therefore, the total interaction, i.e., the confinement, the Coulomb interaction (Hartree and correlation terms) plus the  $sp-d$  interaction results in an inhomogeneous distribution of spin polarization and spin charge density. Holes with parallel spins, at lower density than that of parallel spins, concentrate on the DMS layers, while the latter, at higher density, spreads in a much wider region. The inhomogeneity of the spin polarization density influences the indirect exchange between localized magnetic moments, and this fact is taken into account explicitly in the present calculation. For each value of  $\langle M \rangle$  the exchange interaction terms in Eq. (9) are calculated and tabulated for all possible magnetic ions distances  $R_{ij}$  in the  $(x, y)$  plane according to the zincblende structure within the cutoff radius.

The MC calculation is performed in a finite box, whose axes are parallel to the [100] directions. Its dimensions are  $L_x = L_y$ , and  $L_z = 2L$ , where  $L$  is the width of each DMS layer. Periodic boundary conditions are imposed in the  $(x, y)$  plane. The lateral dimensions are adjusted in such a way that the total number  $N_s$  of Mn sites is about 4000, for all samples with different  $L_z$ . The initial spin orientations of the Mn ions are randomly assigned in the

two DMS layers which are separated by a distance  $d$ , the width of the GaAs spacer. At a given temperature, the energy of the system due to exchange interaction is calculated, and the equilibrium state for a given temperature is sought by changing the individual vector spin orientation according to the Metropolis algorithm.<sup>28</sup> A slow cooling stepwise process is accomplished, starting from above the transition temperature  $T_c$ , and making sure that the thermal equilibrium is reached at every temperature. Every time the net magnetization increases to reach a value of  $n \times 0.1$ ,  $n$  an integer varying from 0 to 10, the tabulated values of the exchange interaction terms are substituted by those corresponding to the new reference  $\langle M \rangle$ . The tabulated values of the exchange interaction terms were calculated from the hole states (eigenfunctions, eigenvalues and Fermi wavevectors) resulting from self-consistent calculation described in Sec. III for this specific thermal average magnetization  $\langle M \rangle$ . Then, the resulting spin configuration for the Mn ions is taken as the starting configuration for the next step at a lower temperature. The Monte Carlo procedure adopted in this way takes account of the changes on the hole gas polarization due to the presence of the established order among the localized magnetic moments in the Mn ions. Thus the magnetization is determined by a fully self-consistent process, but the effects of the fluctuations of the magnetization on the electronic structure are neglected in this process.

For each temperature, the thermal average magnetization  $\langle M \rangle$ , and the Edwards-Anderson (EA) order parameter  $q$  are calculated.<sup>28</sup> The latter is defined as

$$q = \frac{1}{N} \sum_{i=1}^N \left( \sum_{\alpha} \left| \frac{1}{t} \sum_{t'=t_0}^{t_0+t} S_{i\alpha}(t') \right|^2 \right)^{1/2}, \quad (24)$$

where  $\alpha = x, y$  and  $z$ . In order to avoid spurious results on the thermal average values of  $q$  over a large time interval  $t$ , a summation on  $t'$  is performed starting from a time  $t_0$ , when the system already reached the thermal equilibrium. This is true for other quantities such as energy, magnetic susceptibility, etc.

The MC simulations have been performed for several samples as indicated on Table I. The ratio between the carrier concentration and the Mn concentration is the same for the two DMS layers, and is chosen to reproduce hole concentrations which in bulk would be  $p = 1 \times 10^{20} \text{ cm}^{-3}$ , and  $p = 2 \times 10^{20} \text{ cm}^{-3}$ . In Fig. 2 the normalized magnetization as a function of temperature is shown for samples #1 to #6, with the DMS layer width of 10 Å, bulk hole concentration  $p = 1 \times 10^{20} \text{ cm}^{-3}$ , and  $R_c = 5$  monolayers (ML). All these

samples show a paramagnetic (P) to a ferromagnetic (FM) phase transition. The transition temperatures decrease with the increase of the spacer thickness, pointing to the importance of the inter-layer interaction. In Fig. 3 all parameters are kept the same as in the previous figure, but  $p = 2 \times 10^{20} \text{ cm}^{-3}$ . The increase on the hole concentration has two main influences on the magnetization curves: (i) an increase of  $T_c$  and (ii) the possibility of the occurrence of a canted spin phase (C), with a partial ferromagnetic order.<sup>10</sup> This canted spin phase can be explained on the basis of the oscillatory behavior of the exchange interaction. The increase on the hole concentration produces an increase of the Fermi wave number, and anti-ferromagnetic (AF) interactions are likely to occur, according to the oscillatory nature of the (confined) indirect interaction. The Curie temperatures  $T_c$  for samples # 01 to # 12 are obtained in the range from 20 K to 49 K.

In Fig. 4 the results are shown for two 20 Å DMS layers. The hole concentration is  $p = 2 \times 10^{20} \text{ cm}^{-3}$ , and the cutoff length is 5 ML.  $T_c$  decreases with the interlayer separation, as before. However, compared to the 10 Å system, a higher  $T_c$  is observed in the present case. In Fig. 5 the cutoff radius used was 4 ML. We observe here the same behavior as before, but with higher  $T_c$ , and also with higher values of  $\langle M \rangle$ . The presence of effective AF interactions in these samples, due to the oscillatory behavior of the exchange interaction, may produce canted spin phases, rather than FM phases. This results from competing ferro- and antiferromagnetic interactions. It is the case of the so-called frustration. Although these are ordered phases, as can be observed in the EA parameters on Fig. 6, the Mn magnetic moments are not all parallel and the magnetizations at zero temperature are in most samples partial, lying on the range of 60% to 100%. The Curie temperatures  $T_c$  for samples # 13 to # 24 are obtained in the range from 35 to 64 K.

In order to better understand the importance of the spin-polarized indirect exchange on the magnetic order and on the transition temperature of these layered systems, we have compared our results with a simulation performed with an unpolarized exchange. This is done by using the tabulated values of the exchange for  $\langle M \rangle = 0$  in the whole cooling stepwise MC simulation. For this comparison we have chosen a sample with the same characteristics of sample # 1, i.e., two 10 Å DMS layer and a GaAs spacer of 5 Å. The result is shown in Fig. 7. The presence of polarization more than doubles the Curie temperature. This occurs because the effective magnetic potential resulting from the finite thermal average magnetization, and the consequent polarization of the hole gas favor a stronger concentration

of charge and spin on the DMS layers, as can be seen in Fig. 1, providing a stronger exchange than that for the unpolarized system.

A calculation was performed to estimate how the interlayer interaction is affected by the width of the spacer, and how this effect appears in the Curie temperature. To this end, the exchange interaction inside each DMS layer was “turned off” by making it artificially equal to zero. Thus, only the Mn ions belonging to two different DMS layers are interactive. The MC simulations are then performed on the same basis as described before. The results are presented in Table II, for the two DMS layers with 10 Å width separated by 5, 10, 15, 20, 40, and 60 Å, and for two different hole concentrations,  $1 \times 10^{20} \text{ cm}^{-3}$  in Fig. 8 (samples #19 to #24), and  $2 \times 10^{20} \text{ cm}^{-3}$  in Fig. 9 (samples #25 to #30). These results show that there is an effective interlayer coupling able to produce a FM phase. The fact that  $T_c$  coming out exclusively from that interaction is about four times lower than that for the complete interaction reveals that the main contribution to the magnetic ordering within each layer is due to de intralayer coupling. The interlayer interaction acts mainly to establish the ferromagnetic arrangement between the magnetization of the two layers. Notice, however, that the resulting magnetic order affects and is affected by the distribution of charge and spin of the free carriers in the structure. We have performed an exponential fitting of the transition temperature as a function of the spacer thickness for samples with  $L = 10\text{\AA}$ , taking into account the complete interaction and also solely with the interlayer interaction. This is shown in Fig. 10. Notice that the exponential fitting works well in both cases, putting into evidence the importance of the intra-layer interaction. A similar calculation was performed to explore the dependence of the Curie temperature on the DMS layer width, for a fixed spacer thickness ( $d = 10\text{\AA}$ ). The results appear in Fig. 11, for  $L = 10, 20, 40$  and  $50\text{\AA}$ . The Curie temperature increases with the DMS width approaching the fully filled  $T_c$ , as a saturation exponential function.

Up to now the simulations in this work were performed in a single Monte Carlo sample (for each geometry chosen, given by the set of parameters  $L, d$  and  $p$ ) with a specific distribution of the sites occupied by the magnetic ions. Next, the calculation is performed taking into account a configurational average on the initial distribution of the orientation of individual magnetic moments  $\mathbf{S}_i$  on the Mn ions, as well as on the sites  $\mathbf{R}_i$  where these ions are localized. The positions of the Mn ions identify a MC sample. The parameters are chosen as those of sample #01 in Table I. The site configurational average is performed, in each

case, over three initial configurations, namely *a*, *b* and *c* (the MC samples). Although the results do not change significantly, as it can be seen from Fig. 12 which shows the average magnetization *versus* temperature, it is important to observe general behaviors which appear in the process. For instance, Fig. 13 shows the susceptibility *versus* temperature, and we can see that, apart the critical fluctuations to be expected at the transition temperature, which is perfectly defined in that figure, the fluctuations are more important at low temperatures than at high temperatures above  $T_C$ . Another interesting behavior appears in Fig. 14, showing the magnetic specific heat ( $C_V$ ) *versus* temperature. Again, the fluctuations are more important at low temperatures. Besides, the maximum of  $C_V$  occurs at a temperature which is lower than that of the maximum of the susceptibility, what is reminiscent of the spin-glass behavior, and can be understood as a consequence of the competing FM and AF interactions characteristics of the indirect exchange.

## V. DISCUSSIONS AND FINAL COMMENTS

This Monte Carlo simulations shows that this system with two thin GaMnAs layers inside a GaAs matrix presents a ferromagnetic, or at least a canted magnetic phase ordering. The input parameters, namely the hole concentration, the DMS layer width, the DMS layer separation and the interaction cutoff, all influence the magnetic phase of these systems. The increase of hole concentration favors the canted phase due to the intrinsic frustration of the indirect exchange interaction. In the reverse direction, the elimination of the AF interactions produces FM samples and an increase of the  $T_c$  as already observed in a previous work.<sup>10</sup> The increase of the DMS layer width will increase the number of interacting magnetic moments raising also  $T_c$ . As expected,  $T_c$  will be lowered with the increase on the spacer thickness, since as the separation increases the interlayer coupling become weaker and weaker until it reaches a limiting value. This limit is finite due to the confinement by the infinite barriers at the boundaries of the structure. We have quantified the influence of this parameter on the magnetization of the system. Despite the fact that this interlayer interaction is four times weaker than that of the complete system, it is important to notice that it plays an important role in the existence of a FM phase in multilayers, and in digital superlattices.

## Acknowledgments

This work was supported by CENAPAD-SP (Centro Nacional de Processamento de Alto Desempenho em São Paulo) UNICAMP/FINEP-MCT, CNPq and FAPERJ in Brazil, and by the CAPES-COFECUB Franco-Brazilian Program.

---

- <sup>1</sup> J.K. Furdyna and J. Kossut, in *Diluted Magnetic Semiconductors*, edited by J.K. Furdyna and J. Kossut, Semiconductors and Semimetals, Vol. 24, edited by R.K. Willardson and A.C. Beer (Academic Press, N.Y., 1988).
- <sup>2</sup> T. Dietl, in *(Diluted) Magnetic Semiconductors*, edited by T.S. Moss, Handbook of Semiconductors, Vol. 3, edited by S. Mahajan (Elsevier Science B.V., 1994).
- <sup>3</sup> A. Van Esch, L. van Bockstal, J. De Boeck, G. Verbank, A. S. van Steenbergen, P. J. Wellmann, B. Grietens, R. Bogaerts, F. Herlach, and G. Borghs, Phys. Rev. B **56**, 13 103 (1997).
- <sup>4</sup> A. Van Esch, J. De Boeck, L. Van Bockstal, R. Bogaerts, F. Herlach, and G. Borghs, J. Phys.: Condens. Matter **9**, L361 (1997).
- <sup>5</sup> A. Oiwa, S. Katsumoto, A. Endo, M. Hirasawa, Y. Iye, H. Ohno, F. Matsukura, A. Shen, and Y. Sugawara, Solid State Commun. **103**, 209 (1997).
- <sup>6</sup> A. Shen, H. Ohno, F. Matsukura, Y. Sugawara, N. Akiba, T. Kuroiwa, A. Oiwa, A. Endo, S. Katsumoto, Y. Iye, J. Crys. Growth **175/176**, 1069 (1997).
- <sup>7</sup> F. Matsukura, H. Ohno, A. Shen, and Y. Sugawara, Phys. Rev. B **57**, R2037 (1998).
- <sup>8</sup> H. Ohno, N. Akiba, F. Matsukura, A. Shen, K. Ohtani, Y. Ohno, Appl. Phys. Lett. **73**, 363 (1998).
- <sup>9</sup> H. Ohno, F. Matsukura, T. Omiya, and N. Akida, J. Appl. Phys. **85**, 4277 (1999).
- <sup>10</sup> M. A. Boselli, I.C. da Cunha Lima, and A. Ghazali, Phys. Rev. B **62**, 8895 (2000).
- <sup>11</sup> T. Dietl, H. Ohno, and F. Matsukura, Phys. Rev. B **63**, 195205 (2001); T. Dietl *et al*, Physica E **7**, 967 (2000).
- <sup>12</sup> T. Jungwirth W. A. Atkinson, B. H. Lee, and A. H. MacDonald, Phys. Rev. B **59**, 9818 (1999); B. Lee, T. Jungwirth, and A. H. MacDonald, Phys. Rev. B **61**, 15606 (2000).
- <sup>13</sup> Malcolm P. Kennett, Mona Berciu and R. N. Bhatt, Phys. Rev. B **65**, 115380 (2002).
- <sup>14</sup> T. Dietl, H. Ohno, F. Matsukura, J. Cibert, and D. Ferrand, Science **287**, 1019 (2000); see also

the special issue of *Semicond. Sci. Technol.* **17** (2002).

<sup>15</sup> I. Ya. Korenblit and E.F. Shender, Sov. Phys. JETP **42**, 566 (1975).

<sup>16</sup> C. Kittel, in *Solid State Physics*, edited by F. Seitz, D. Turnbull, and H. Ehrenreich (Academic Press, N.Y., 1968), Vol. 22.

<sup>17</sup> Ulf Larsen, Phys. Lett. **85A**, 471 (1981).

<sup>18</sup> M. T. Béal-Monod, Phys. Rev. B **36**, 8788 (1987).

<sup>19</sup> U. Gummich and I. C. da Cunha Lima, Solid State Commun. **76**, 831 (1990).

<sup>20</sup> D. N. Aristov, Phys. Rev. B **55**, 8064 (1997).

<sup>21</sup> J. S. Helman and W. Baltensperger, Phys. Rev. B **50**, 12 682 (1994).

<sup>22</sup> J. S. Helman and W. Baltensperger, Phys. Rev. B **53**, 275 (1996).

<sup>23</sup> L. Loureiro da Silva, M. A. Boselli, I. C. da Cunha Lima, X. F. Wang, and A. Ghazali, Appl. Phys. Lett. **79** 3305 (2001).

<sup>24</sup> A. A. Abrikosov, L.P. Gorkov, and I. E. Dzyaloshinsky, *Methods of Quantum Field Theory in Statistical Physics*, edited by Richard A. Silverman (Dover , 1963).

<sup>25</sup> L. V. Keldysh, D.A. Kirzhnitz, and A. A. Maradudin, editors, *The Dielectric Function of Condensed Systems* (Elsevier Science B. V., North-Holland, 1989).

<sup>26</sup> M. A. Boselli, I. C. da Cunha Lima, and A. Ghazali, J. Appl. Phys. **85**, 5944 (1999).

<sup>27</sup> J. Okabayashi, A. Kimura, O. Rader, T. Mizokawa, A. Fujimori, T. Hayashi, and M. Tanaka, Phys. Rev. B **58**, R4211 (1998).

<sup>28</sup> H. T. Diep, A. Ghazali, and P. Lallemand, J. Phys. C: Solid State Phys. **18**, 5881 (1985).

FIG. 1: (a) Structure model used in the present calculation: two DMS layers inside a GaAs quantum. (b) The effective magnetic potential (schematic). (c) Density distribution: charge(solid line), spin polarization(dashed), anti-parallel spin (dashed-dotted), and parallel spin (dotted).

FIG. 2: Normalized magnetization *vs* temperature for samples #01 to #06 indicated in Table I.

FIG. 4: Normalized magnetization *vs* temperature for samples #13 to #18 indicated in Table I.

FIG. 5: Normalized magnetization *vs* temperature for samples #19 to #24 indicated in Table I.

FIG. 6: Edward-Anderson order parameter *vs* temperature for samples #13 to #18 indicated in Table I.

FIG. 7: Comparison for the polarized (solid line) and unpolarized (dotted line) system. The characteristics of the sample are the same as sample #01, indicated in Table I.

FIG. 8: Normalized magnetization *vs* temperature for samples #25 to #30 indicated in Table II taking into account only the interlayer interaction.

FIG. 9: Normalized magnetization *vs* temperature for samples #31 to #36 indicated in Table II taking into account only the interlayer interaction.

FIG. 10: Curie temperature *vs* spacer thickness for  $L = 10\text{\AA}$ , and  $p = 1. \times 10^{20} \text{ cm}^{-3}$  for the complete interaction (samples #01 to #06 indicated in Table I) and for the interlayer interaction (samples #25 to #30 indicated in Table II). An exponential fitting  $y(x) = y_0 + A \exp(-x/\lambda)$  is shown, with the resulting parameters:  $y_0 = 20.1\text{K}$ ,  $A = 31.2\text{K}$ ,  $\lambda = 9.8\text{\AA}$  for the complete interaction;  $y_0 = 5.9\text{K}$ ,  $A = 15.4\text{K}$ ,  $\lambda = 6.5\text{\AA}$  for the interlayer interaction.

FIG. 11: Curie temperature *vs* DMS layer thickness for  $d = 10\text{\AA}$ , and  $p = 2. \times 10^{20} \text{ cm}^{-3}$  An exponential fitting  $y(x) = y_0(1 - \exp(-x/\lambda))$  is shown, with the resulting parameters:  $y_0 = 85.4\text{K}$ , and  $\lambda = 15.2\text{\AA}$ .

FIG. 3: Same as Fig 2 for samples #07 to #12 indicated in Table I.

TABLE I: Sample characteristics: L is the width of each DMS layer; d is the GaAs spacer width; the ratio of the carrier concentration to the Mn concentration, written in terms of a bulk hole concentration,  $p$  ;  $T_c$  is the transition temperature for phases: FM: ferromagnetic, C: canted spin;  $R_c$  is the cutoff radius of the exchange interaction in number of monolayers.

sample	L (Å)	d (Å)	r	$R_c$	phase	$T_c$ (K)
#01	10	05	1	5	FM	38
#02	10	10	1	5	FM	31
#03	10	15	1	5	FM	28
#04	10	20	1	5	FM	23
#05	10	40	1	5	FM	21
#06	10	60	1	5	FM	20
#07	10	05	2	5	C	49
#08	10	10	2	5	FM	39
#09	10	15	2	5	FM	35
#10	10	20	2	5	FM	34
#11	10	40	2	5	FM	32
#12	10	60	2	5	FM	22
#13	20	05	2	5	C	62
#14	20	10	2	5	C	63
#15	20	15	2	5	C	59
#16	20	20	2	5	C	59
#17	20	40	2	5	C	53
#18	20	60	2	5	C	51
#19	20	05	2	4	FM	64
#20	20	10	2	4	FM	56
#21	20	15	2	4	FM	52
#22	20	20	2	4	FM	49
#23	10	40	2	4	FM	35
#24	10	60	2	4	FM	45

TABLE II: Same as table 1, but considering only interlayer interaction.

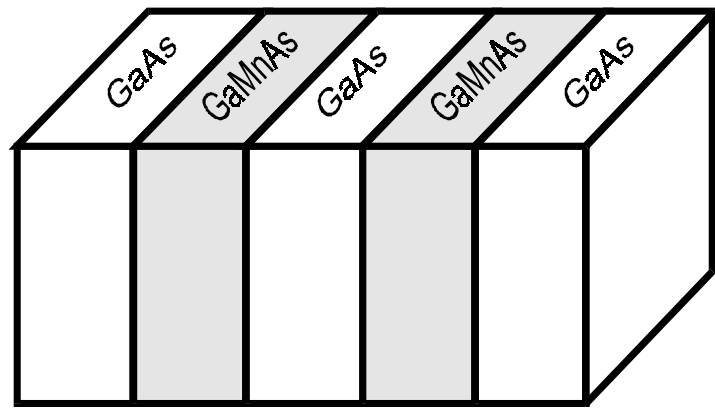
sample	L (Å)	d (Å)	$p$ ( $10^{20}$ cm $^{-3}$ )	$R_c$	phase	$T_c$ (K)	
#25	10	05		1	5	FM	13
#26	10	10		1	5	FM	09
#27	10	15		1	5	FM	08
#28	10	20		1	5	FM	06
#29	10	40		1	5	FM	06
#30	10	60		1	5	FM	06
#31	10	05		2	5	FM	15
#32	10	10		2	5	FM	08
#33	10	15		2	5	FM	08
#34	10	20		2	5	FM	08
#35	10	40		2	5	FM	08
#36	10	60		2	5	FM	07

FIG. 12: Thermal average magnetization as a function of temperature for three different magnetic moments configurations (open symbols), and the corresponding configurational average (solid square), corresponding to the parameters of sample #01.

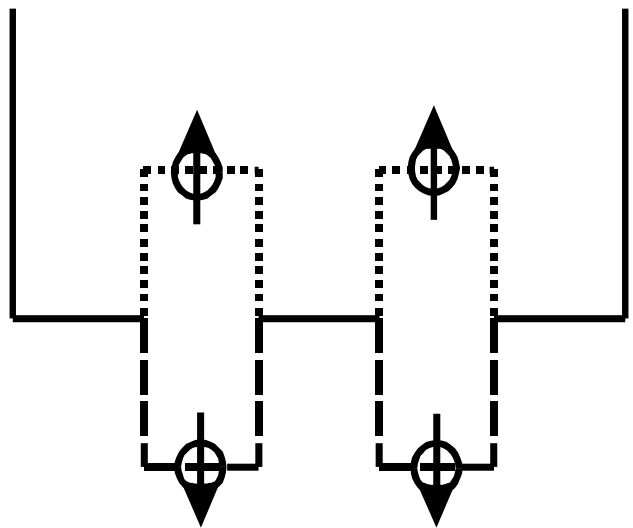
FIG. 13: Magnetic susceptibility *vs* temperature, calculated from thermal fluctuations, for three different magnetic moments configurations (open symbols), and the corresponding configurational average (solid square), corresponding to the parameters of sample #01.

FIG. 14: Magnetic specific heat *vs* temperature, calculated from thermal fluctuations, for three different magnetic moments configurations (open symbols), and the corresponding configurational average (solid square), corresponding to the parameters of sample #01.

(a)



(b)



(c)

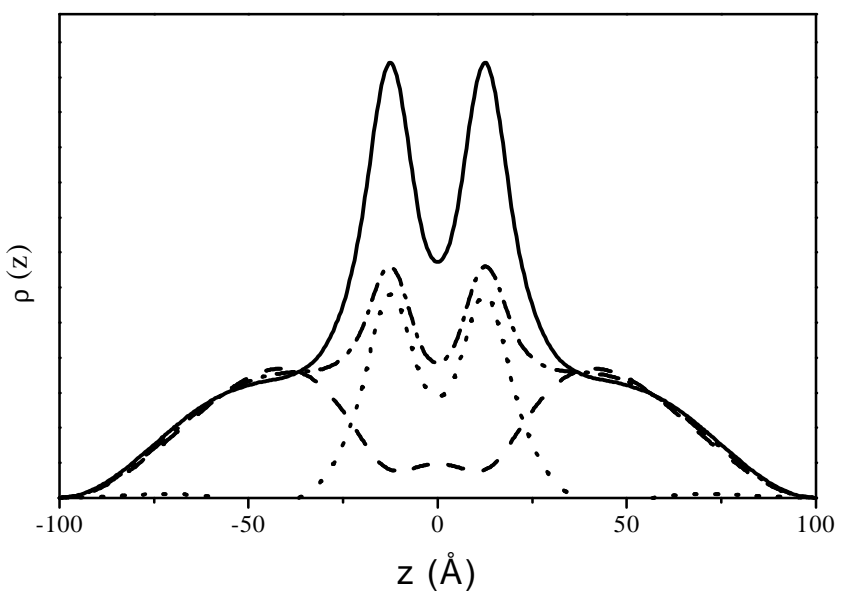


Fig. 01 Boselli *et al.*

fig. 02 Boselli *et al.*

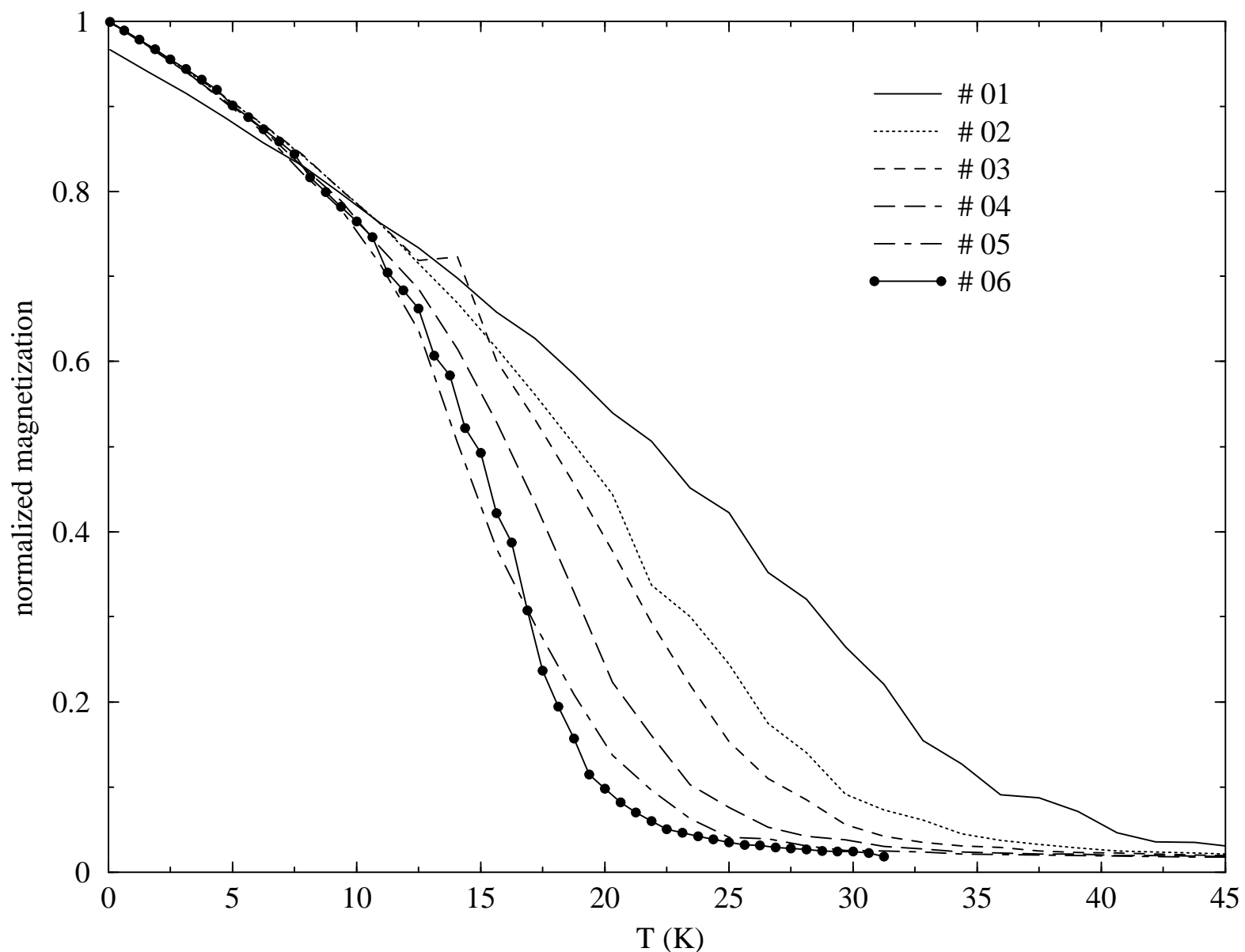


fig. 03 Boselli *et al.*

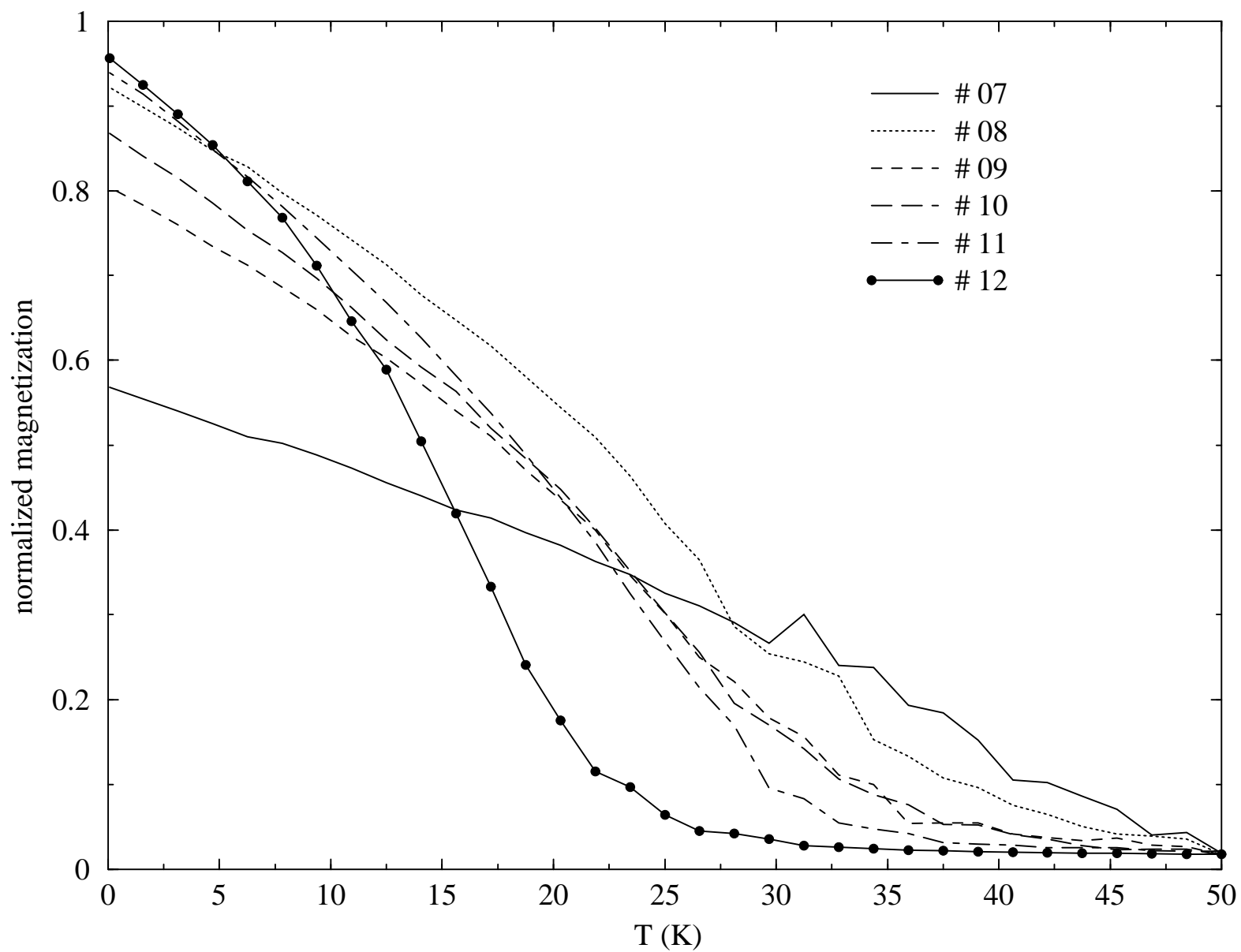


fig. 04 Boselli *et al.*

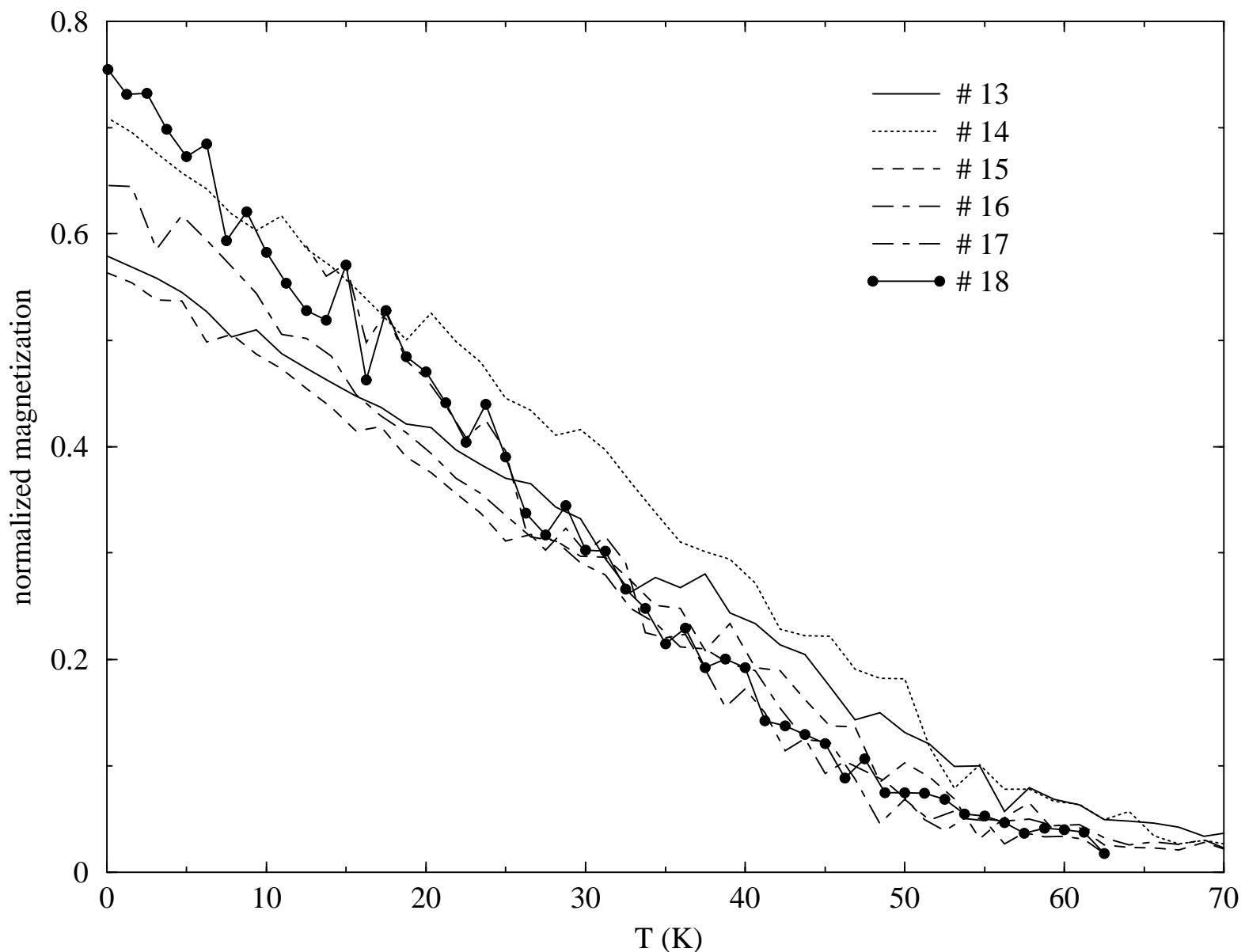


fig. 05 Boselli *et al.*

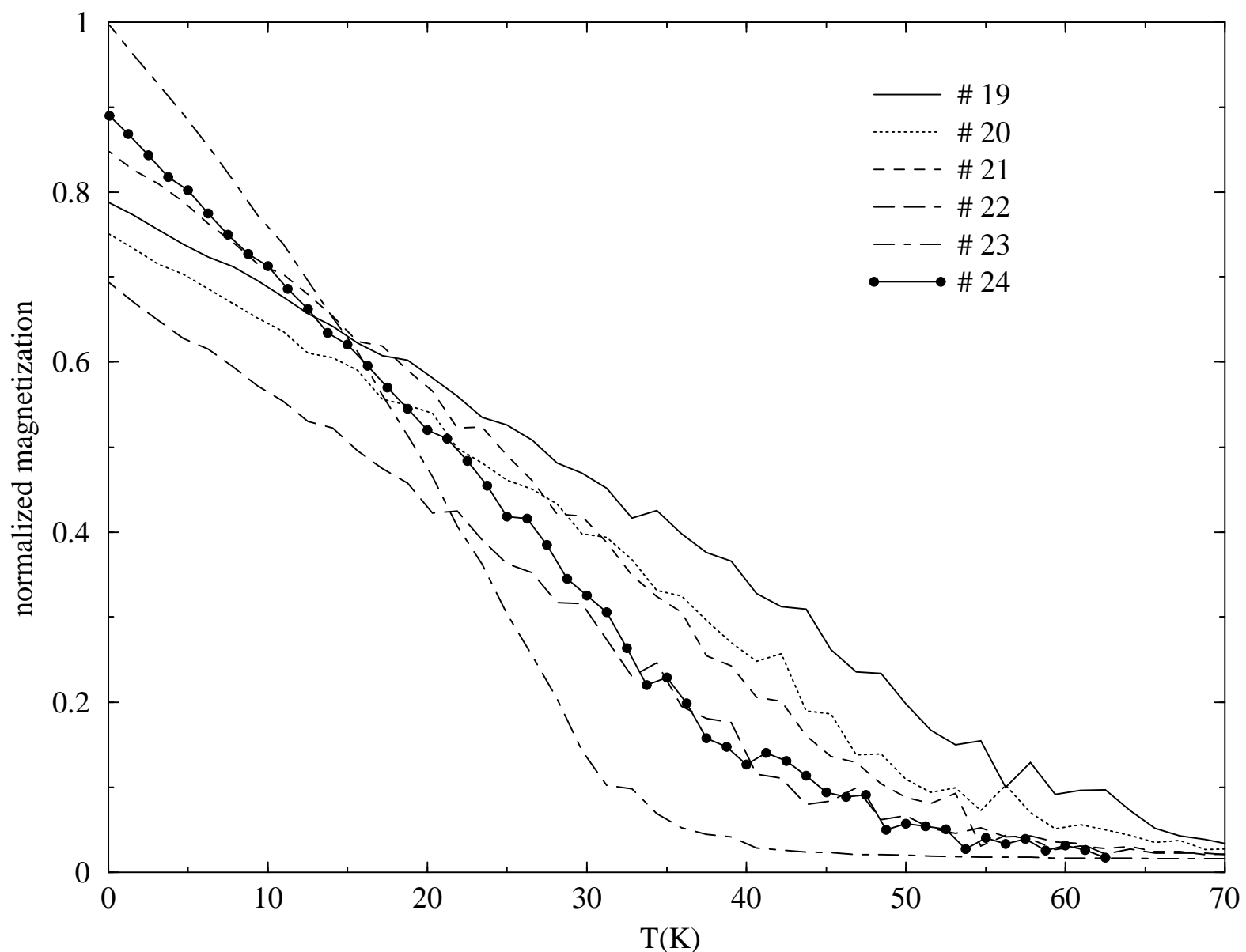


fig. 06 Boselli *et al.*

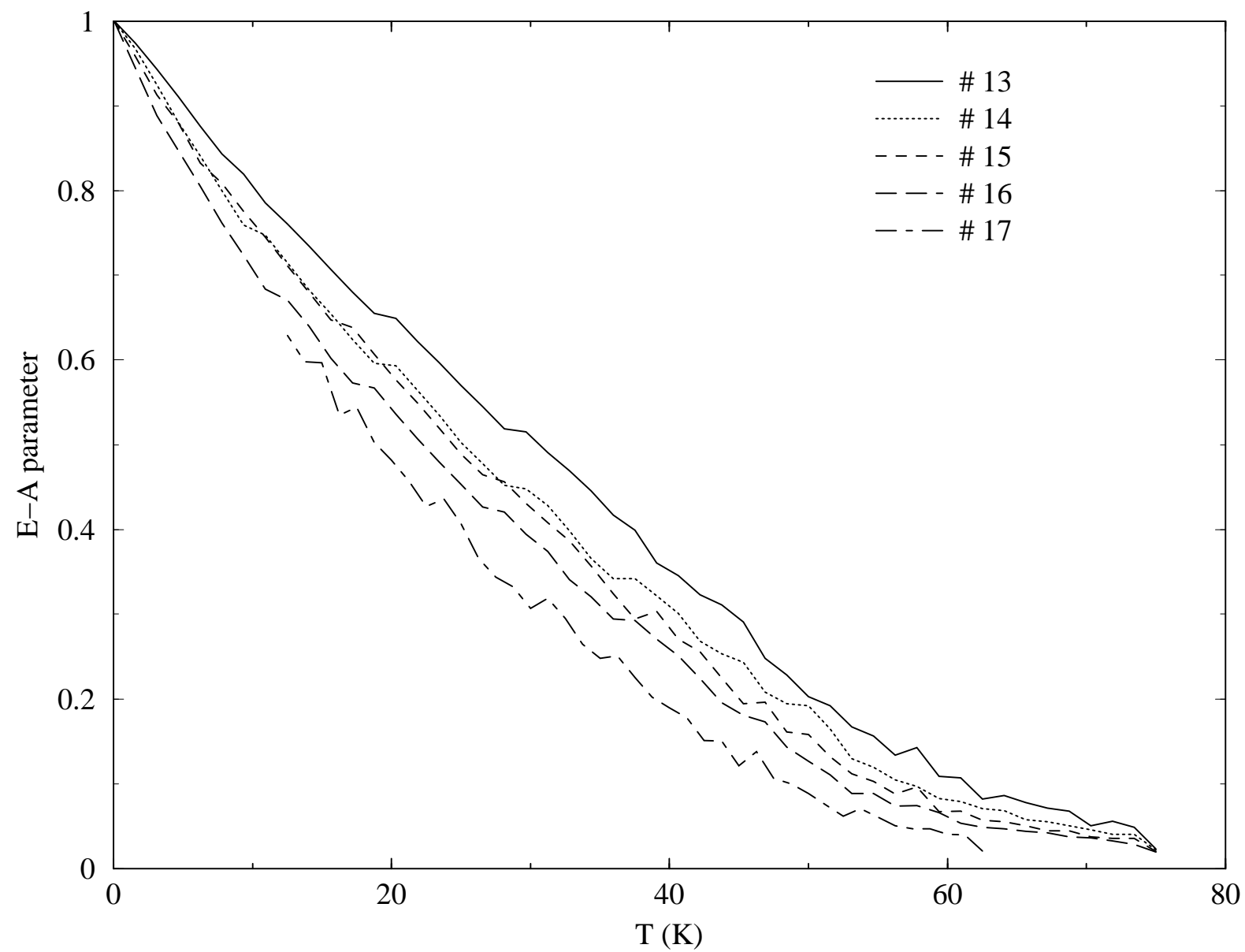


Fig. 07 Boselli, *et al.*

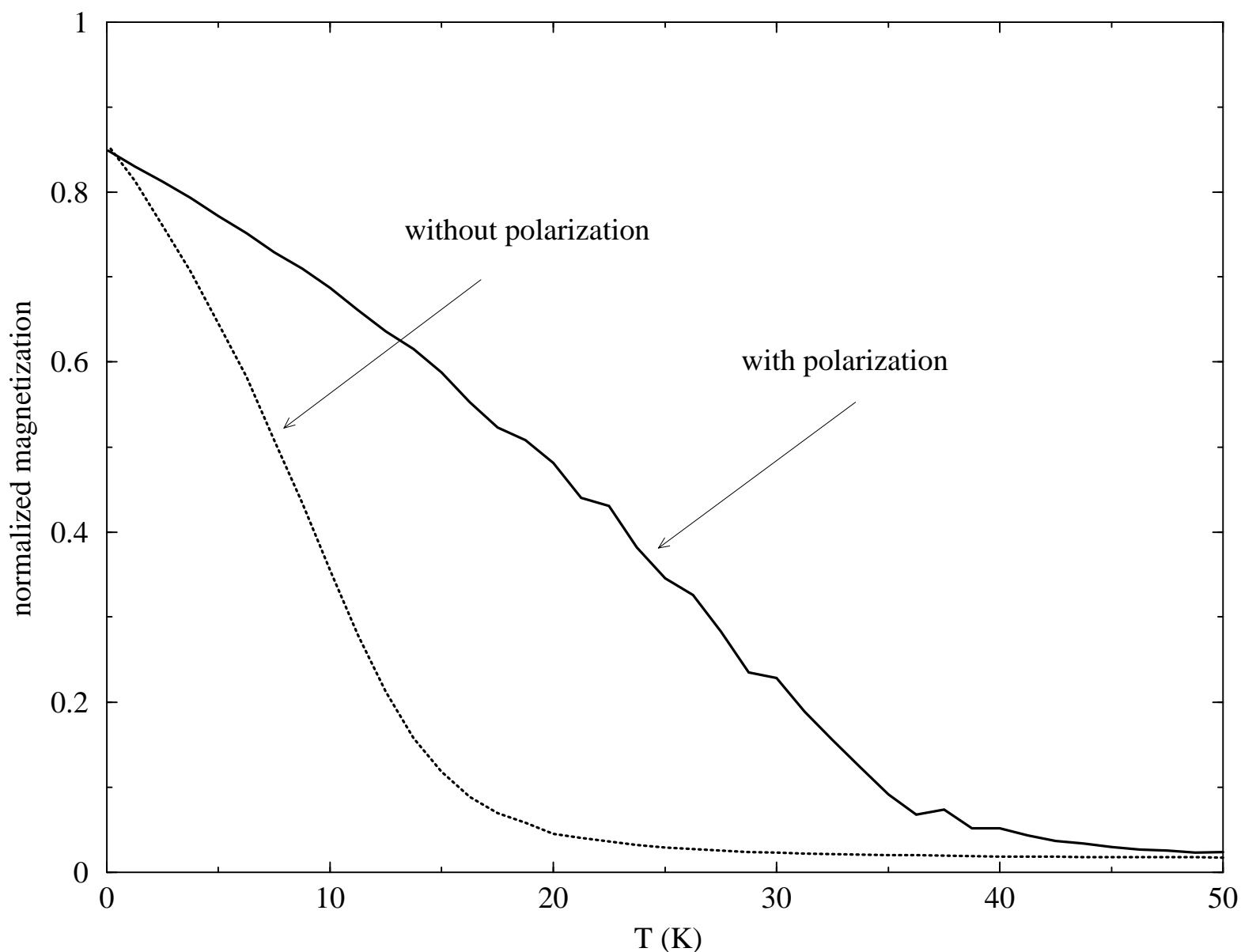


fig. 08 Boselli *et al.*

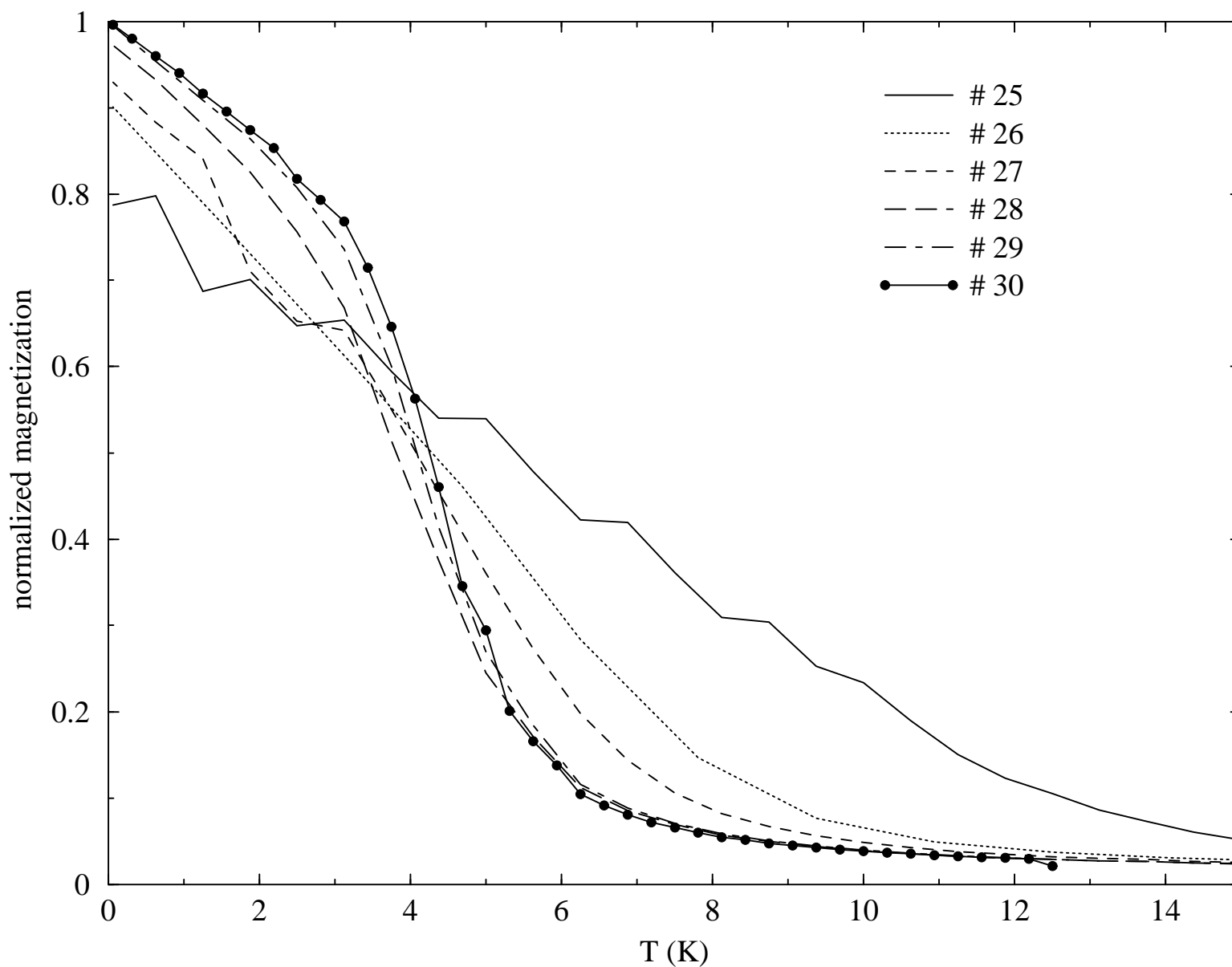


fig. 09 Boselli *et al.*

